

Research Article

Static and Dynamic Properties and Temperature Sensitivity of Emulsified Asphalt Concrete

Bin Huang ¹, Yuting Zhang ¹, Tian Qi,² and Hongxing Han¹

¹School of Civil Engineering, Wuhan University, No. 8 East-Lake South Road, Wuhan, China

²Guangzhou Environmental Protection Investment Group Co., Ltd., Guangzhou, China

Correspondence should be addressed to Yuting Zhang; zhangytwhu@163.com

Received 17 November 2017; Revised 1 April 2018; Accepted 6 May 2018; Published 10 June 2018

Academic Editor: Baozhong Sun

Copyright © 2018 Bin Huang et al. This is an open access article distributed under the Creative Commons Attribution License, which permits unrestricted use, distribution, and reproduction in any medium, provided the original work is properly cited.

Asphalt concrete is a typical rheological material, which is hard brittle at low temperature and reflects soft plastic failure at high temperature; the temperature has a great influence on the mechanical properties of asphalt concrete. In order to eliminate the environmental pollution caused by hot asphalt construction, cationic emulsified asphalt can be used. This paper transforms the temperature control system for static and dynamic triaxial test equipment, which has achieved static and dynamic properties of emulsified asphalt concrete under different temperatures, and researched the temperature sensitivity of emulsified asphalt concrete materials including static stress-strain relationship, static strength, dynamic modulus of elasticity, damping ratio, and so on. The results suggest that (1) temperature has a great influence on the triaxial stress-strain relationship curve of the asphalt concrete. The lower the temperature, the greater the initial tangent modulus of asphalt concrete and the higher the intensity; the more obvious the softening trend, the smaller the failure strain of the specimen and the more obvious the extent of shear dilatancy. When the temperature is below 15.4°C, the temperature sensitivity of the modulus and strength is stronger significantly. (2) With the temperature rising, the asphalt concrete gradually shifts from an elastic state to a viscoelastic state, the dynamic modulus gradually reduces, and the damping ratio increases. When the temperature is above 15.4°C, the temperature sensitivity is obviously stronger for the dynamic elastic modulus and damping ratio. (3) The static and dynamic properties of asphalt concrete are very sensitive to the temperature. The test temperature should be made clear for the static and dynamic tests of asphalt concrete. The specimen temperature and the test ambient temperature must be strictly controlled.

1. Introduction

Asphalt concrete is made of asphalt, aggregate, filler, and other cement together to form a synthetic material, is the material more and more widely used in transportation and water conservancy projects, and has an important social and economic value. In order to eliminate the shortcomings of traditional hot asphalt construction heating and environmental pollution, we consider the use of nonheated emulsified asphalt. For the porosity and short storage time of the conventional emulsified asphalt concrete, as well as the difficult to have the fatigue strength, surface closure requirements, and other deficiencies, the use of cationic emulsified asphalt was considered.

Highway traffic load, seasonal difference, climate difference, cold area and hot zone, sunshine and reservoir water temperature differences, and other factors have the impact of asphalt concrete engineering properties [1–6]. Asphalt concrete is a typical rheological material. It has different constitutive characteristics under long-term load and cyclic load, and it exhibits hardness and brittleness at low temperature. It reflects soft plasticity at high temperature, and the effect of temperature and static force on the mechanical properties of asphalt concrete is very big.

Based on the static and dynamic triaxial test of emulsified asphalt concrete under different temperatures, this paper has researched the temperature sensitivity of static stress-strain

TABLE 1: The mix proportion of asphalt concrete.

| Asphalt- aggregate ratio (%) | Aggregate gradation (%) | | | | Cement | Mineral powder |
|------------------------------------|-------------------------|------|-----|---------------|--------|-------------------|
| | 10-20 | 5-10 | 3-5 | 0.075-3 mm | | |
| 6.7 | 10 | 21 | 25 | 38 | 3 | 3 |

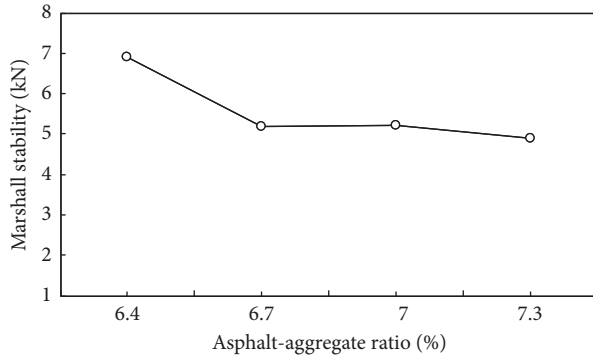


FIGURE 1: Relation curve of Marshall stability and asphalt-aggregate ratio.

relationship, static strength, dynamic modulus of elasticity, and damping ratio for emulsified asphalt concrete materials. Also, it provided the basis for temperature reliability evaluation of material with emulsified asphalt concrete.

2. Static Triaxial Test

2.1. Testing Methods. We used cationic emulsified asphalt in this test, and the solid content is 52%. The density is 1.01 g/cm^3 , penetration is 95.5 mm, ductility is 160 cm, and the softening point is 43.2°C . The mineral aggregate is crushed dolomite; the padding is ore powder of dolomite and PO42.5 cement. The mix proportion of asphalt concrete test is shown in Table 1.

The mixture ratio of aggregates and fillers is preliminarily determined by the dense skeleton stacking test [7], and then the asphalt content test is designed to analyze the influence of bituminous stone ratio on Marshall stability, flow value, and porosity of asphalt concrete, so as to determine the best mixture ratio. The relationship between Marshall stability, flow value, porosity, and oil stone ratio is shown in Figures 1-3. In terms of these three factors, the performance of oil and stone is better when the ratio of oil and stone is 6.7%.

The mixing material is treated with microwave before compaction, so that the emulsified asphalt is completely demulsified and the water in the emulsified asphalt is evaporated by maintaining the temperature at $120\sim 130^\circ\text{C}$. The molded specimen is subjected to a static test on a triaxial apparatus. There is no drainage during the test, and the use of body variable measurement is required rather than an external body. Temperature has a great influence on the mechanical property of the asphalt concrete, so we need to control the sample temperature in the process of the triaxial test. The temperature of the asphalt concrete triaxial test is

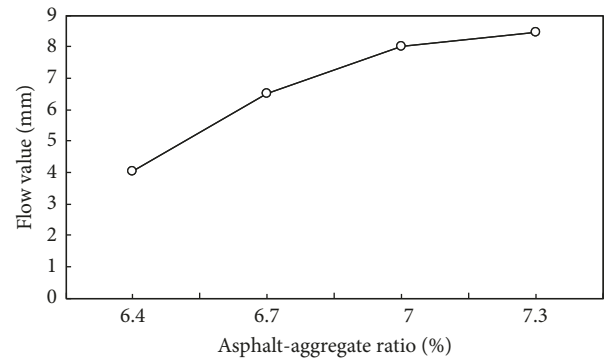


FIGURE 2: Relation curve of flow value and asphalt-aggregate ratio.

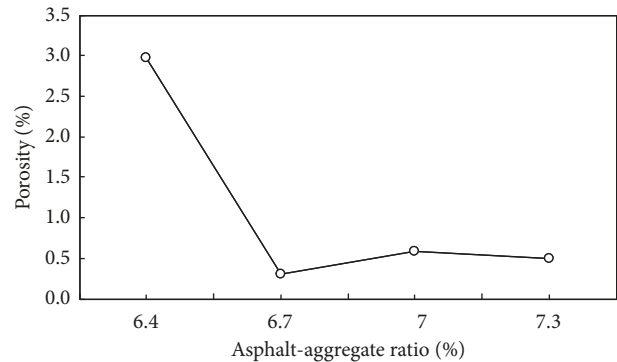


FIGURE 3: Relation curve of porosity and asphalt-aggregate ratio.

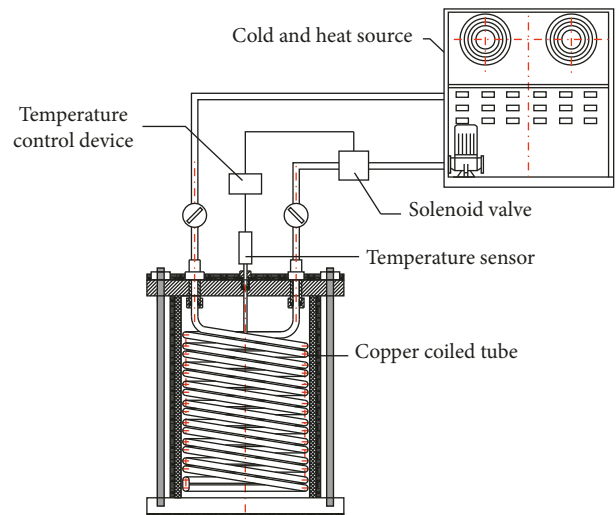


FIGURE 4: The static triaxial temperature control system.

controlled by the copper coiled tube between the inside wall and outside wall of the pressure chamber. The copper coiled tube is filled with freezing liquid, and it is circulating all the time. And a temperature sensor is placed inside the pressure chamber to monitor the water temperature. The thermostat solenoid valve controls the water temperature to keep $\pm 0.5^\circ\text{C}$ range of the test temperature [8]. The triaxial temperature control system is shown in Figure 4.

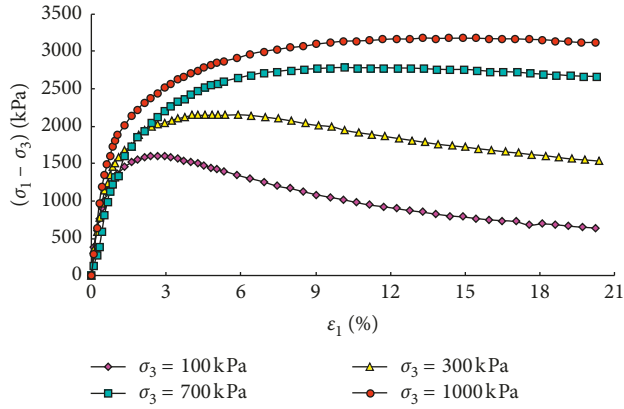


FIGURE 5: The relationship between stress and strain ($T = 5.4^{\circ}\text{C}$).

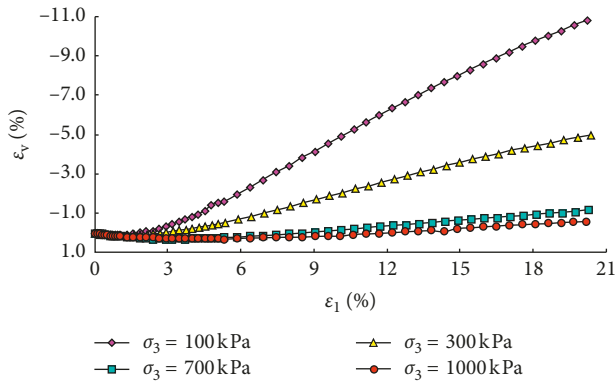


FIGURE 6: The relationship between volumetric strain and strain ($T = 5.4^{\circ}\text{C}$).

The specimens are molded by using the compaction method. The asphalt concrete whose mix proportion is shown in Table 1 is tested on the static triaxial apparatus at 5.4, 15.4, and 25.4°C. The specimens are kept in water bath at constant temperature for 24 hours before the test. The specimen size is $\Phi 101 \text{ mm} \times H200 \text{ mm}$, and the porosity is 1.9%. The cell pressures of the test are 0.1, 0.3, 0.7, and 1.0 MPa, and the shearing rate is 1.0 mm/min.

2.2. Temperature Sensibility of Stress-Strain Relationship.

The typical stress-strain and volumetric strain-strain relationship of the asphalt concrete are shown in Figures 5 and 6. We can see that the asphalt concrete shows softening at low cell pressure, and its failure strain is small. But with the increase of cell pressure, it shows gradual hardening, and the destruction of deviatoric stress increased significantly and failure strain is also larger. At the beginning of the test, the volume change-strain curves showed shear contraction and followed dilatation. The performance of shear dilatation is more apparent: at lower cell pressure, the dilatancy is more obvious.

Asphalt concrete is a typical rheological material, and the temperature has a significant impact on its mechanical properties. Figure 7 shows the stress-strain relationship

curve under the same cell pressure at different temperature conditions. Table 2 shows the results of destruction strain under different temperatures and cell pressures. Table 3 shows the $E-\mu$ model [9] parameters of the triaxial test under different temperatures. The results can be seen as follows:

- (1) When the temperature is under 15.4°C , the stress-strain relationship curves are grossly softening, and the temperature has a great influence on the initial tangent modulus and the failure strain. But when the temperature is over 15.4°C , the stress-strain relationship curves show hardening type, and it significantly reduced the temperature sensitivity of initial tangent modulus and failure strain.
- (2) At low temperatures (5.4°C), the initial phase of the stress-strain relationship curves for the asphalt concrete is steeper, It means the initial tangent modulus is greater, and the softening phenomenon is more obvious, especially when the cell pressure is low, and the corresponding failure strain is small ($<5\%$). But at higher temperature conditions (25.4°C), the asphalt concrete shows hardening phenomenon, the failure strain is increased by 7%, and the initial tangent modulus significantly reduced compared to that at lower temperature. It is only 25% of low modulus or less.
- (3) As the temperature decreases, the steeper the initial stages of asphalt concrete stress-strain curve are, the higher the initial tangent modulus is. The lower the temperature is, the more obvious the softening phenomenon is and the smaller the failure strain of the sample is.

The temperature also has a great influence on the volumetric strain of asphalt concrete. Figure 8 shows the volume change-strain curve under the same cell pressure but at different temperatures. As the test results show, under high pressure ($\geq 700 \text{ kPa}$) and temperature conditions (25.4°C), the volume change curve of asphalt concrete shows shear contraction, but with the reducing pressure and temperature, the curve is gradually changed to shear dilatation, especially under lower temperature (5.4°C) and cell pressure ($\leq 300 \text{ kPa}$), with almost no shear shrinkage. The differences of volume strain corresponding to the same axial strain are up to 8%.

2.3. Temperature Sensibility of Static Strength.

The asphalt concrete has a peak point under low temperature and low cell pressure. It takes the peak point as the asphalt concrete strength if the peak appears during the test, but if peak does not appear, it takes the partial stress which corresponds to the axial strain of 20% as asphalt concrete strength. Figure 9 shows the relationship of destruction deviator stress and the test temperature. It can be learned from Figure 7 that the higher the temperature, the lower the strength of asphalt concrete. But the influence of temperature on strength at low and high confining pressures is not identical. When the cell pressure is 0.7 MPa and 1.0 MPa, the strength of asphalt

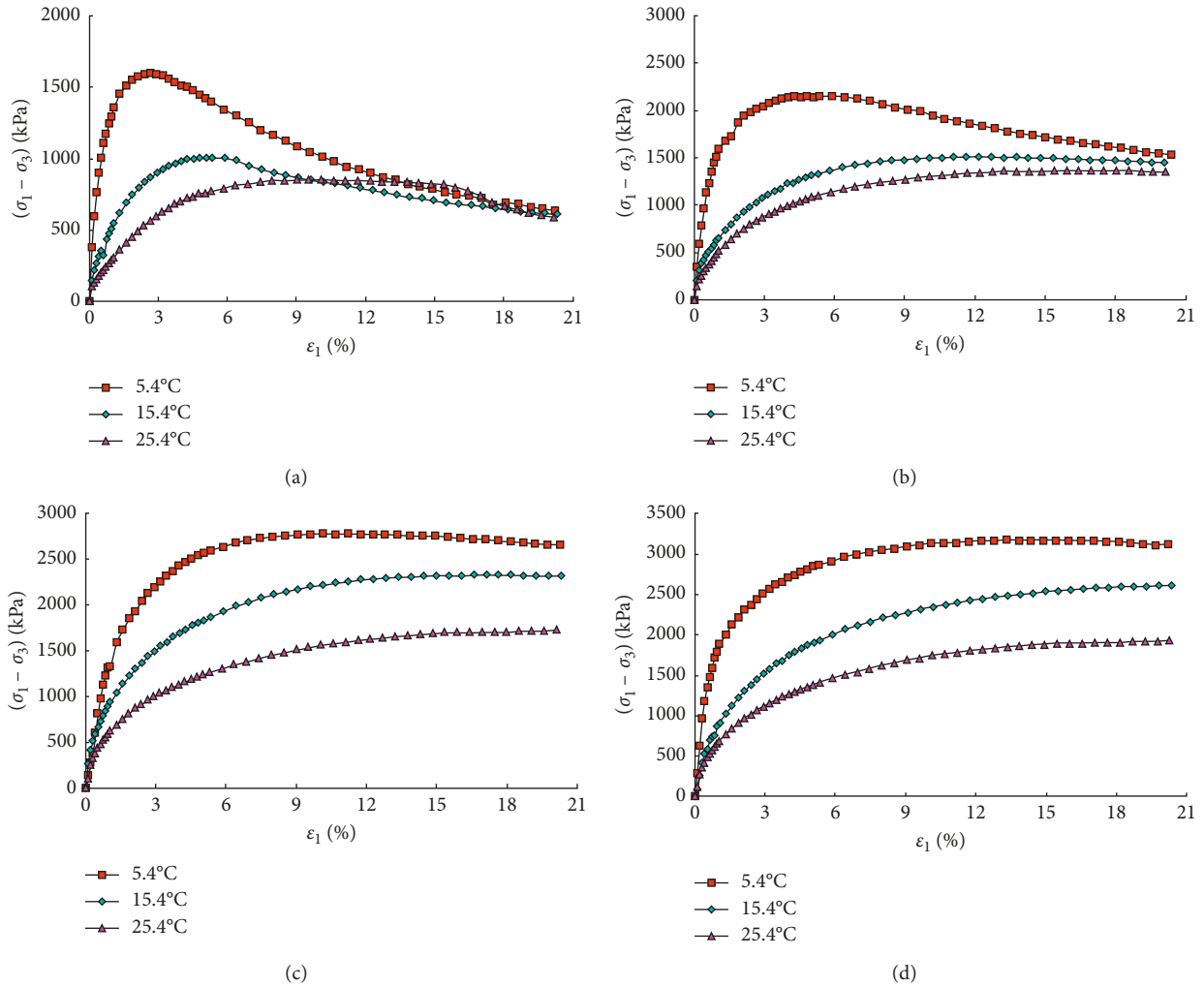


FIGURE 7: The relationship between stress and strain. (a) $\sigma_3 = 0.1$ MPa, (b) $\sigma_3 = 0.3$ MPa, (c) $\sigma_3 = 0.7$ MPa, and (d) $\sigma_3 = 1.0$ MPa.

TABLE 2: The results of failure strain.

| T ($^{\circ}\text{C}$) | Failure strain (%) | | | |
|----------------------------|--------------------|------|------|------|
| | 100 | 300 | 700 | 1000 |
| 5.4 | 2.66 | 5.89 | 10.1 | 13.3 |
| 15.4 | 5.34 | 12.2 | 17.1 | 20.0 |
| 25.4 | 10.1 | 18.6 | 20.0 | 20.0 |

TABLE 3: The triaxial test $E-\mu$ model parameters.

| T ($^{\circ}\text{C}$) | K | n | R_f | G | F | D |
|----------------------------|--------|-------|-------|-------|-------|-----|
| 5.4 | 2096.0 | 0.202 | 0.888 | 0.594 | 0.143 | 0 |
| 15.4 | 738.2 | 0.212 | 0.890 | 0.529 | 0.090 | 0 |
| 25.4 | 500.5 | 0.202 | 0.897 | 0.481 | 0.040 | 0 |

concrete almost decreased linearly, and when the confining pressure is 0.1 MPa and 0.3 MPa, the destruction of deviator stress happens, and test temperature curve is steep if the temperature is rising from 5.4°C to 15.4°C, but the curve is gentle if the temperature is rising from 15.4°C to 25.4°C, consistent with the existing research [3]. At high temperature, the lower the cell pressure, the smaller influence of the temperature on strength.

Figure 10 shows Mohr's stress circles of triaxial tests of asphalt concrete under different temperatures ($T = 5.4^{\circ}\text{C}$, 15.4°C , and 25.4°C). Table 4 shows the strength parameters of the triaxial test. It can be seen that the temperature increased from 5.4°C to 15.4°C, the cohesion dropped rapidly, and the angle of internal friction had no big change. And

temperature increased from 15.4°C to 25.4°C, the cohesion change was small, and internal friction angle declined largely, reducing the temperature to 7.1°C. In general, when the temperature is below 15.4°C, the temperature sensitivity of strength is significant.

2.4. Comparison between Normal Asphalt Concrete (NAC) and Cationic Emulsified Asphalt Concrete (CEAC). The comparison of the triaxial test strength at different temperatures are shown in Figure 11, and the results of the triaxial test strength failure strain at different temperatures are shown in Figure 12. At the temperature of 5.4°C, the CEAC specimen strength is higher than that of NAC specimen, but the law is opposite at the temperature of

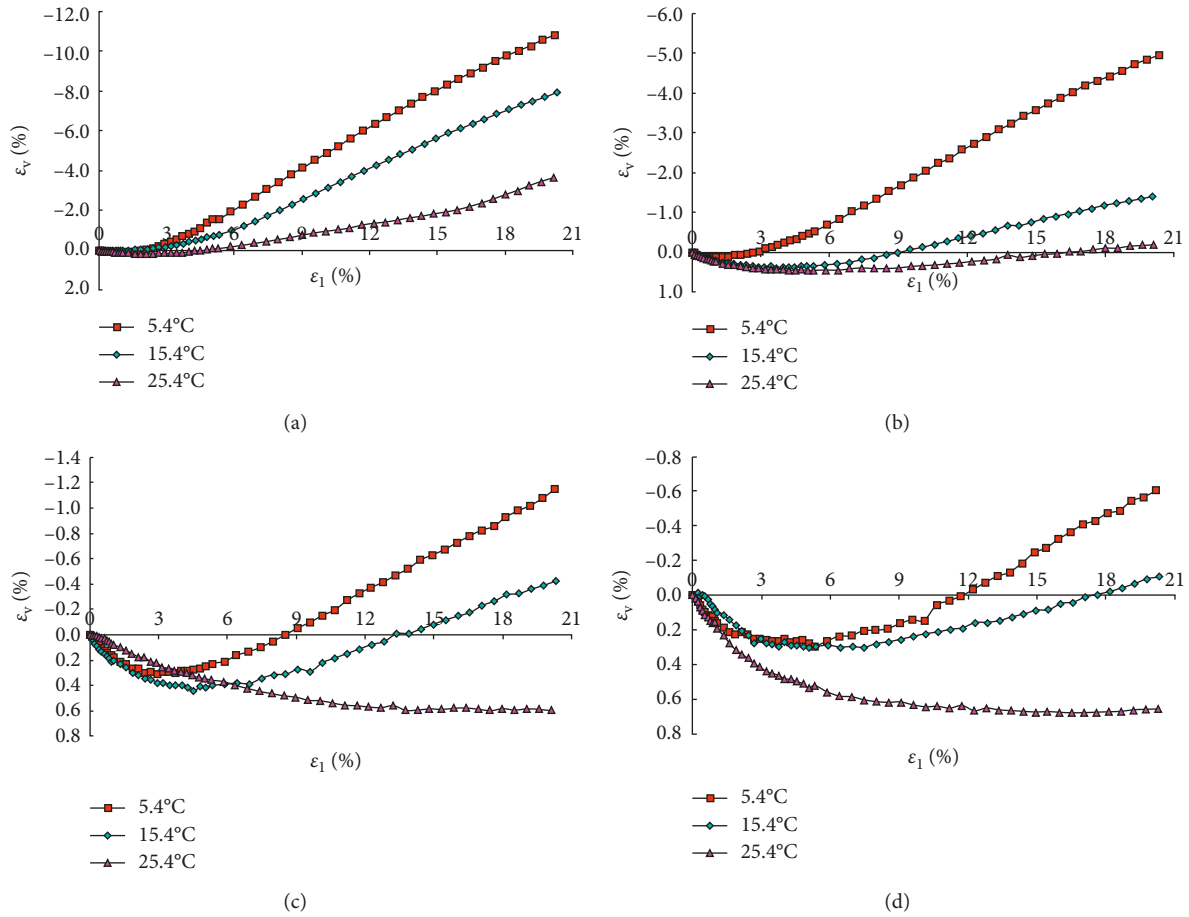


FIGURE 8: The relationship between volumetric strain and strain under different temperatures. (a) $\sigma_3 = 0.1$ MPa, (b) $\sigma_3 = 0.3$ MPa, (c) $\sigma_3 = 0.7$ MPa, and (d) $\sigma_3 = 1.0$ MPa.

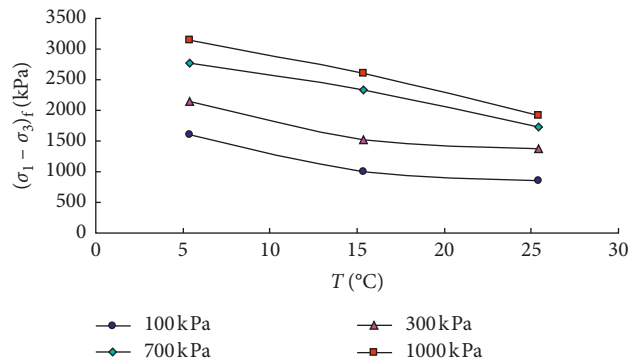


FIGURE 9: The relationship between destruction deviator stress and temperature.

25.4°C; at the temperature of 15.4°C, under low confining pressure, the strength of NAC is higher, and when the confining pressure is large, the strength of CEAC is higher. Therefore, the strength of CEAC specimen is greatly influenced by temperature, and the temperature sensitivity is stronger. Compared with the NAC, the failure strain of the CEAC specimen is smaller, especially at low temperature, and its adaptability to deformability is worse. In conclusion, CEAC has higher strength at medium and low temperatures,

but for the temperature sensitivity and deformation ability of asphalt concrete, NAC is better. CEAC can improve temperature sensitivity and deformation ability by adding modifiers [10].

3. Dynamic Triaxial Test

3.1. Testing Methods. The test material is the same as the static triaxial tests. The triaxial test of asphalt concrete is

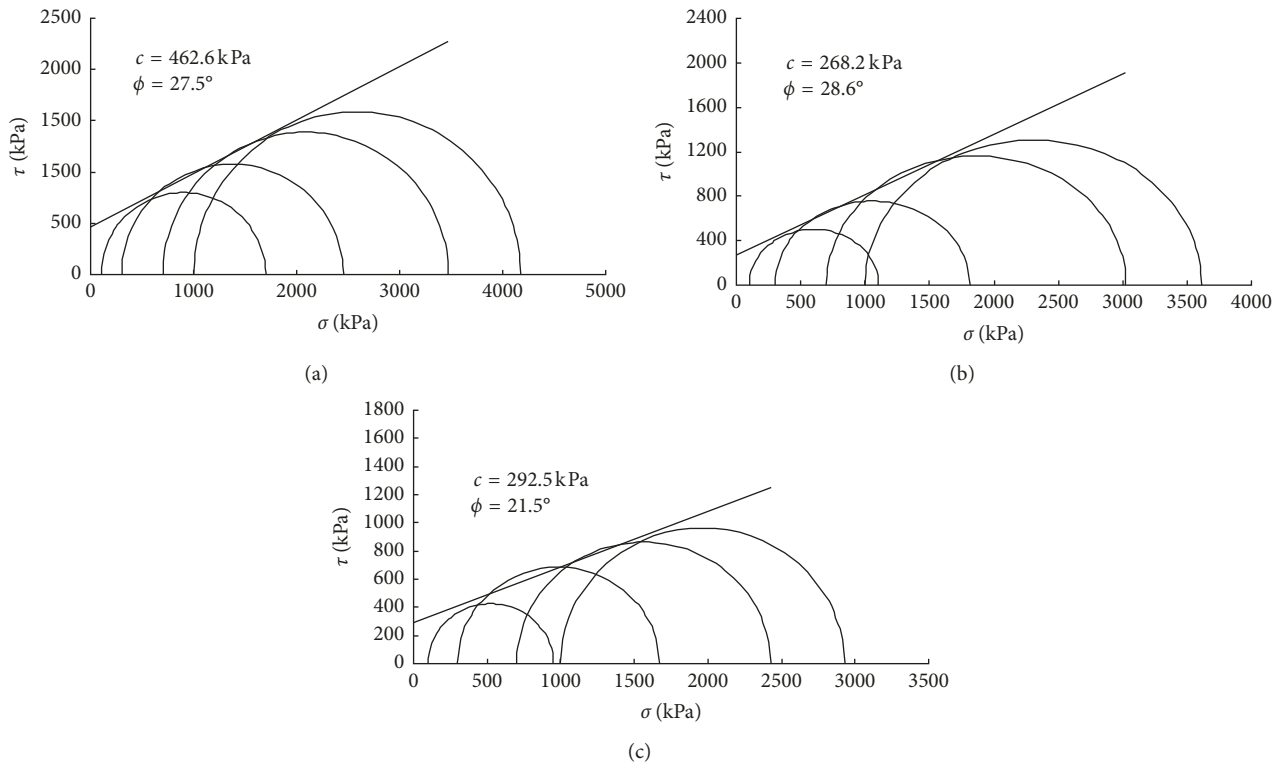


FIGURE 10: Mohr's stress circles of triaxial tests of asphalt concrete. (a) $T = 5.4^\circ\text{C}$, (b) $T = 15.4^\circ\text{C}$, and (c) $T = 25.4^\circ\text{C}$.

TABLE 4: Triaxial test strength parameters.

| T ($^\circ\text{C}$) | c (kPa) | Φ ($^\circ$) |
|--------------------------|-----------|---------------------|
| 5.4 | 462.5 | 27.5 |
| 15.4 | 268.2 | 28.6 |
| 25.4 | 292.5 | 21.5 |

performed on the dynamic triaxial apparatus, and the specimen size is $\Phi 101 \text{ mm} \times H 200 \text{ mm}$. In order to control test temperature, the pressure chamber has been modified. A copper tube is installed between outside the sample and the inwall of the pressure chamber, and it controls pressure chamber temperature by circulation of the internal water in the copper during the test. Figure 13 shows the testing apparatus.

The asphalt concrete triaxial tests conducted three groups test at three different temperatures of 5.4°C , 15.4°C , and 25.4°C , and the trial confining pressures are 300 kPa, 600 kPa, 900 kPa, and 1200 kPa. Specimens are put in water bath at a constant temperature which is the test temperature for 24 hours before the test and then installing the specimen on the dynamic triaxial apparatus. The pressure chamber is filled airless with water at the test temperature, while the water is starting to circulate in the copper tube. After installation, the sample is applied at ambient pressure and the drain valve is opened to let the specimen be in contact with the atmosphere. After it is applied, it should be maintained at a constant pressure for 30 minutes before starting the dynamic test. The dynamic load is sinusoidal and vibrates five times under each load, and the vibration frequency is 1 Hz.

3.2. The Temperature Sensitivity of Elastic Modulus and Damping Ratio. Under the same temperature conditions, when the dynamic strain of asphalt concrete materials is $10^{-4} \sim 10^{-3}$, the elastic modulus variation is small (the modulus change does not exceed 16.3% at the same temperature, the same confining pressure, and the same consolidation ratio), and the damping ratio is also small (≤ 0.11); it is substantially an elastic deformation phase. The dynamic stress-dynamic strain backbone curve of asphalt concrete basically showed a linear relationship. The dynamic strain has little influence on the dynamic modulus, and it can fit the dynamic stress-dynamic strain backbone curve of the asphalt concrete triaxial test by a straight line through the origin [11]. Figure 14 shows the typical backbone curve, and the linear correlation coefficient of fitting is over 0.99, so that the slope can be taken as a dynamic modulus of asphalt concrete. The elastic modulus of asphalt concrete is shown in Table 5. (The stress ratio (α) is obtained by σ_1 (initial axial pressure) and σ_3 (initial confining pressure), $\alpha = \sigma_1/\sigma_3$.)

Figure 15 shows the relationship curve of dynamic modulus and temperature. The higher curve is the temperature, and the lower one, the dynamic modulus. But under different cell pressures, the effect of temperature on the dynamic modulus is different. The lower the cell pressure, the steeper the relationship curve of dynamic modulus and temperature, at the temperature of $15.4^\circ\text{C} \sim 25.4^\circ\text{C}$. The higher the temperature, the greater the impact on dynamic modulus. In general, when the temperature is higher than 15.4°C , the temperature sensitivity of dynamic modulus was significantly stronger, but this is just opposite of the static modulus law.

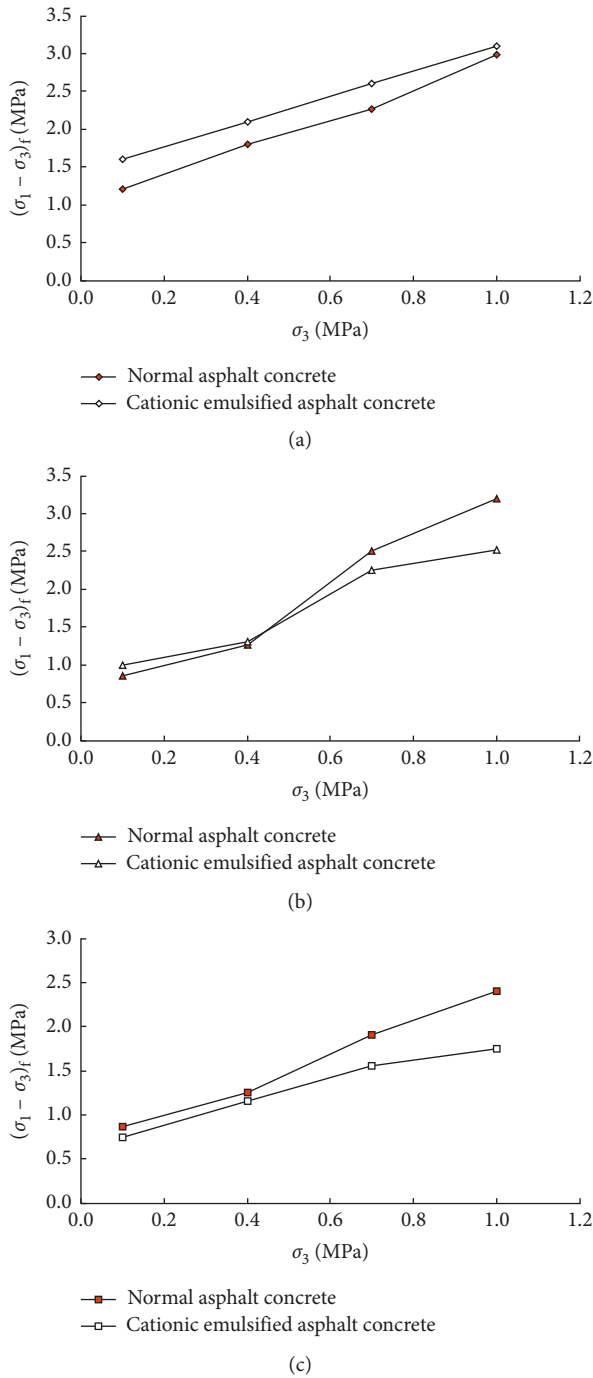


FIGURE 11: Triaxial test strength comparison of normal asphalt and cationic emulsified asphalt concrete. (a) $T = 5.4^\circ\text{C}$, (b) $T = 15.4^\circ\text{C}$, and (c) $T = 25.4^\circ\text{C}$.

Figure 16 shows the typical curve of damping ratio and dynamic strain of asphalt concrete. Under different experimental conditions, the damping ratio range of asphalt concrete is from 0.02 to 0.11, while under the same experimental conditions, the damping ratio changes very little with the increase of dynamic strain. Until now, there is no formula of empirical calculation about the relationship of damping ratio and dynamic strain of the asphalt concrete dynamic triaxial test. In accordance with “Hydraulic asphalt concrete testing

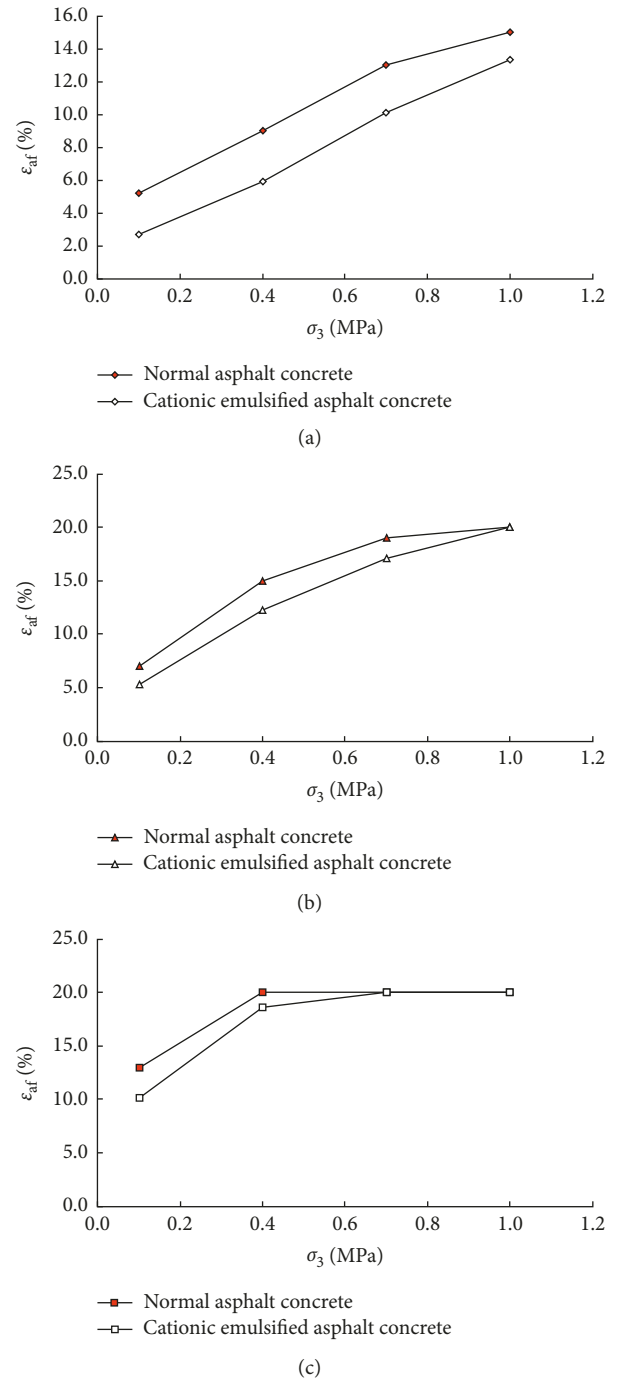


FIGURE 12: Triaxial test failure strain comparison of normal asphalt and cationic emulsified asphalt concrete. (a) $T = 5.4^\circ\text{C}$, (b) $T = 15.4^\circ\text{C}$, and (c) $T = 25.4^\circ\text{C}$.

regulations” (DL/T 5362-2006) [12], the average of damping ratio is the damping ratio, so this paper takes the average as the damping ratio of asphalt concrete. The results of asphalt concrete damping ratio are shown in Table 6.

Figure 17 shows the relationship between damping ratio of asphalt concrete and temperature. The higher the temperature, the greater the damping ratio of asphalt concrete, but the influence of temperature on the damping ratio is not the same under high temperature and low temperature. The curve of

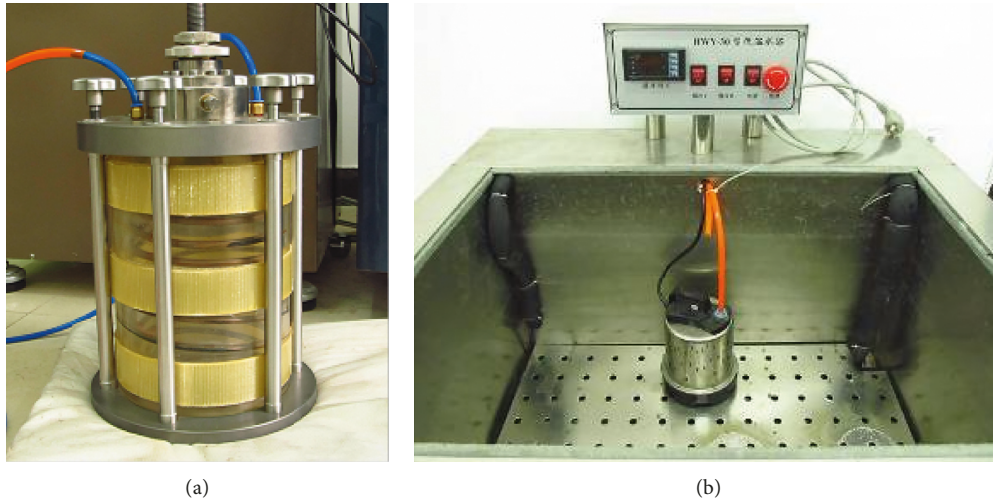


FIGURE 13: The temperature control system.

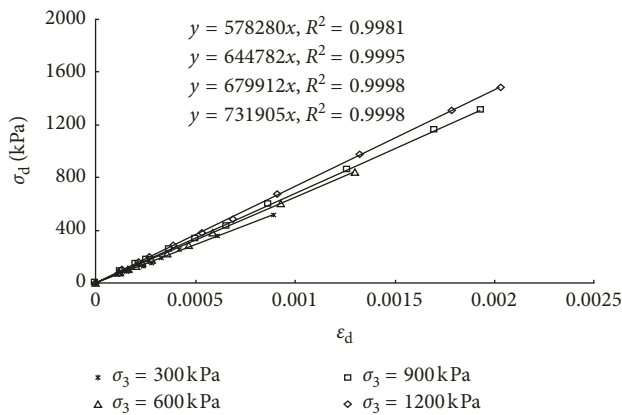


FIGURE 14: The backbone curves of the dynamic triaxial test ($T = 5.4^{\circ}\text{C}$, $K_c = 1.5$).

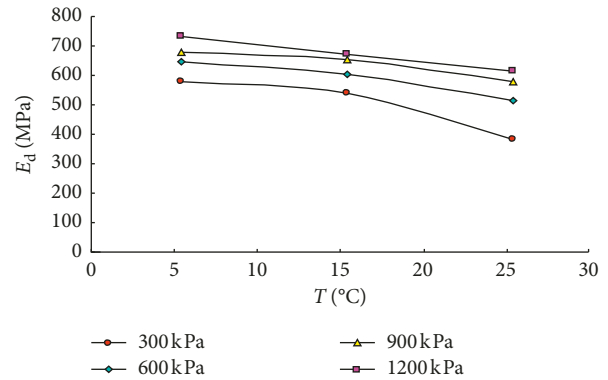


FIGURE 15: The relationship between dynamic modulus and temperature.

TABLE 5: The dynamic modulus results.

| T ($^{\circ}\text{C}$) | Stress ratio | Dynamic modulus (MPa) | | | |
|----------------------------|--------------|-----------------------|-----|-----|------|
| | | 300 | 600 | 900 | 1200 |
| 5.4 | 1.5 | 578 | 645 | 680 | 732 |
| 15.4 | 1.5 | 539 | 604 | 652 | 671 |
| 25.4 | 1.5 | 381 | 515 | 580 | 614 |

damping ratio and temperature relationship is steep at the higher temperature section ($15.4^{\circ}\text{C} \sim 25.4^{\circ}\text{C}$). The higher the temperature, the greater the effect of temperature on damping ratio. In general, when the temperature is over 15.4°C , the temperature sensitivity of damping ratio was significantly stronger, and it coincides with the dynamic modulus law.

4. Conclusions

The researches presented in this paper can be summarized as follows:

- (i) When the temperature is under 15.4°C , the stress-strain curves are substantially softening, and the temperature has a great influence on the initial

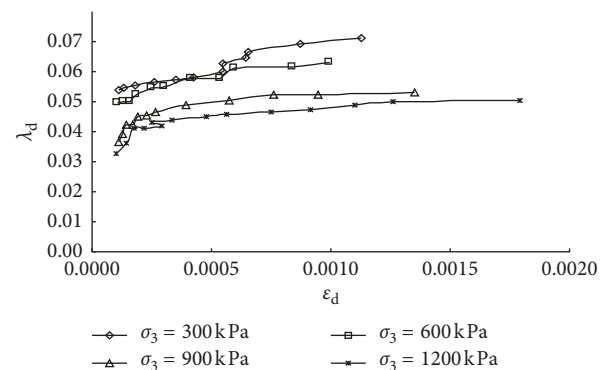


FIGURE 16: The relationship between damping ratio and dynamic strain.

TABLE 6: The damping ratio results.

| T ($^{\circ}\text{C}$) | Stress ratio | Damping ratio | | | |
|----------------------------|--------------|---------------|-------|-------|-------|
| | | 300 | 600 | 900 | 1200 |
| 5.4 | 1.5 | 0.061 | 0.049 | 0.044 | 0.037 |
| 15.4 | 1.5 | 0.072 | 0.060 | 0.045 | 0.040 |
| 25.4 | 1.5 | 0.094 | 0.074 | 0.063 | 0.052 |

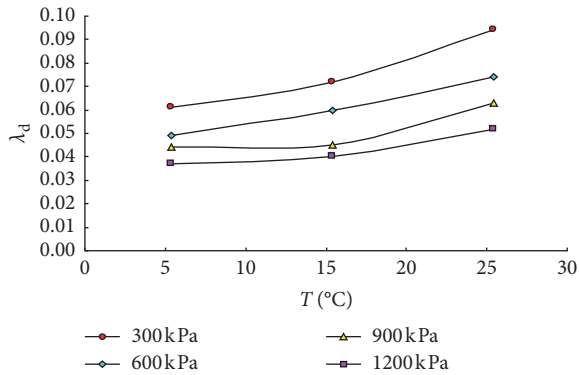


FIGURE 17: The relationship between damping ratio and temperature.

tangent modulus and the failure strain. While the temperature is over 15.4°C, the stress-strain curves are substantially hardened, and the temperature sensibility of initial tangent modulus and the failure strain is significantly reduced.

- (ii) At low temperature, the initial tangent modulus is large and the softening phenomenon is obvious, especially when the confining pressure is low, and the corresponding failure strain is small; while at the high temperature conditions, asphalt concrete is hardened, failure strain increases largely, and initial tangent modulus relatively decreases compared to that at low temperature.
- (iii) When the pressure and the temperature decreases, the body change curves gradually transform into dilatancy, especially at low temperatures and low confining pressure, almost no shear contraction; the volumetric strain of the same axial strain is different because of temperature.
- (iv) When the temperature is under 15.4°C, the temperature sensibility of static strength and modulus is significantly stronger, but when the temperature is over 15.4°C, the temperature sensibility of dynamic modulus is strong, which is contrary to the law of static modulus.
- (v) When the temperature increases from 5.4°C to 15.4°C, the cohesion of the static strength indicator drops sharply, but the angle of internal friction of static strength index has little difference; while the temperature increases from 15.4°C to 25.4°C, the cohesion of the static strength indicator has little difference; however, the angle of internal friction of static strength index drops largely.

Conflicts of Interest

The authors declare that they have no conflicts of interest.

Acknowledgments

This research was financially supported by the National Natural Science Foundation of China (Grant nos. 51309028 and 51378403).

References

- [1] J. J. Feng, Y. X. Ge, and Z. X. Sun, "Experimental study on stress-strain relationship of asphalt concrete," *Journal of Hydraulic Engineering*, vol. 11, pp. 56–62, 1987.
- [2] S. Feizi-Khankandi, A. A. Mirghasemi, A. Ghalandarzadeh, and K. Kaare Hoeg, "Cyclic triaxial tests on asphalt concrete as a water barrier for embankment dams," *Soils and Foundations*, vol. 48, no. 3, pp. 319–332, 2008.
- [3] Y. Chen, T. Jiang, Z. Q. Huang et al., "Effect of temperature on mechanical properties of asphalt concrete," *Rock and Soil Mechanics*, vol. 31, no. 7, pp. 2192–2196, 2010.
- [4] J. C. Guo, "Triaxial tests and stress-strain characteristics of asphalt concrete," *Water Resources and Hydropower Engineering*, vol. 9, pp. 58–64, 1981.
- [5] W. B. Wang, Z. T. Sun, and L. Y. Wu, "Study on stress-strain characteristics of asphalt concrete," *Journal of Hydraulic Engineering*, vol. 5, pp. 1–8, 1996.
- [6] Z. Q. Li, H. R. Zhang, and Y. F. Hou, "Triaxial test study on mechanical characteristics of asphalt concrete in the core wall of earth-rock fill dam," *Chinese Journal of Rock Mechanics and Engineering*, vol. 25, no. 5, pp. 997–1002, 2006.
- [7] Q. J. Ding, X. L. Huang, H. X. Wang, C. Z. Huang, and Q. Jing, "Adopt the method of dense proportion design to produce high-performance concrete with high fii volume," *Concrete*, vol. 29, no. 8, pp. 7–10, 2007.
- [8] B. Huang, Z. L. Cheng, X. B. Rao et al., *A High-Low Temperature Controlling Equipment of Triaxial Tests*, 201420144307.4 [P], China, 2014.
- [9] J. M. Duncan, *Strength, Stress-Strain and Bulk Modulus Parameters for Finite Element Analyses of Stresses and Movements in Soil Masses*, University of California, Berkeley, CA, USA, 1980.
- [10] B. Huang, X. Y. Wu, and F. Tan, "Experimental study on mechanics characteristics of hydraulic asphalt concrete," in *Proceedings of the Technology for Earth-Rockfill Dam 2012*, Dandong, pp. 476–481, 2012.
- [11] W. Wang, K. Hoeg, and M. Asce, "Cyclic behavior of asphalt concrete used as impervious core in embankment dams," *Journal of Geotechnical and Geoenvironmental Engineering*, vol. 137, no. 5, pp. 536–544, 2011.
- [12] DL/T 5362-2006, *Hydraulic Asphalt Concrete Testing Regulations*, China Electric Power Press, Beijing, China, 2006.



Hindawi
Submit your manuscripts at
www.hindawi.com

